



Hydrodynamic research on flap-type WEC with high accuracy coupled SPH method

Shi Yingxuan
Zhejiang University

Contents

One

Background

Two

Methodology

Three

Results and discussions

Four

Conclusions

Contents

One
background

Two
Methodology

Three
Results& discussions

Four
Conclusions



Background

Contents

One background

Wave energy is important not only for alleviating energy crisis but also supplying the power for **islands**.

For improving efficiency of wave energy capturing, it is important to study **hydrodynamic characteristics** of floating.

Two Methodology

Three Results& discussions

Four Conclusions



Contents

One

background

Two

Methodology

Three

Results& discussions

Four

Conclusions



Methodology

Contents

One
background

Two
Methodology

Three
Results& discussions

Four
Conclusions

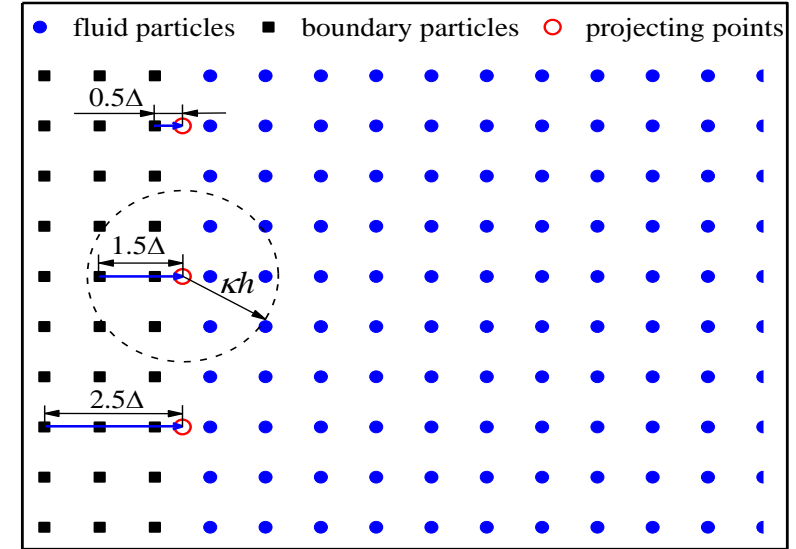
Discrete governing equations

$$\begin{cases} \frac{D\rho_i}{Dt} = \rho_i \sum_j (\mathbf{u}_i - \mathbf{u}_j) \cdot \nabla_i W_{ij} V_j + \rho_{\delta i} \\ \rho_i \frac{D\mathbf{u}_i}{Dt} = - \sum_j (p_i + p_j) \cdot \nabla_i W_{ij} V_j + \rho_i \mathbf{g} + \boldsymbol{\tau}_i \\ \frac{D\mathbf{x}_i}{Dt} = \mathbf{u}_i \\ p_i = (\rho_i - \rho_r) c^2 \end{cases}$$

δ -SPH model

$$\begin{cases} \rho_\delta = \delta h c_0 \sum_j \psi_{ij} \nabla_i W_{ij} V_j \\ \psi_{ij} = 2(\rho_i - \rho_j) \frac{\mathbf{x}_i - \mathbf{x}_j}{|\mathbf{r}_{ij}|^2} - [\langle \nabla p \rangle_i^L + \langle \nabla p \rangle_j^L] \\ \langle \nabla p \rangle_i^L = \sum_j (\rho_i - \rho_j) L_i \nabla_i W_{ij} V_j \\ L_i = \sum_j (\mathbf{x}_i - \mathbf{x}_j) \otimes \nabla_i W_{ij} V_j \\ \boldsymbol{\tau}_i = \alpha h c_0 \rho_0 \sum_j \frac{(\mathbf{u}_j - \mathbf{u}_i) \cdot (\mathbf{r}_j - \mathbf{r}_i)}{|\mathbf{r}_j - \mathbf{r}_i|^2} \nabla_i W V_j \\ \nu = \frac{\alpha h c_0}{2(d+2)} \end{cases}$$

Boundary condition



1、Motionless walls

$$p_b = p_p - \rho_0 \mathbf{g} \cdot \mathbf{n}_b \eta \Delta$$

$$\begin{cases} u_b^n = -u_p^n \\ u_b^\tau = u_p^\tau \end{cases}$$

2、Moving boundary

$$p_b = p_p - \rho_0 \left[\frac{D\mathbf{u}_b}{Dt} \cdot \mathbf{n}_b + \mathbf{g} \cdot \mathbf{n}_b \right] \eta \Delta$$

Contents

One background

Two Methodology

Three Results& discussions

Four Conclusions

Wave-maker theory

$$x_{\text{piston}}(t) = \frac{s}{2} \sin(\sigma t)$$

$$s = H/(kd)$$

Boundary force model

$$f_{ij} = \begin{cases} - \left(c_0 \frac{(\mathbf{u}_i - \mathbf{u}_j) \cdot \mathbf{n}_j W_{ij} h_{ij}^d \mathbf{n}_j}{|\mathbf{r}_{ij} \cdot \mathbf{n}_j|} \right) & (\mathbf{u}_i - \mathbf{u}_j) \cdot \mathbf{n}_j < 0 \\ 0 & (\mathbf{u}_i - \mathbf{u}_j) \cdot \mathbf{n}_j \geq 0 \end{cases}$$

The motions of floating body

$$\begin{cases} \mathbf{F} = \sum_{i \in \text{solid}} \frac{D\mathbf{u}_i}{Dt} \\ \mathbf{T} = \sum_{i \in \text{solid}} \frac{D\mathbf{u}_i}{Dt} (\mathbf{x}_i - \mathbf{x}_{\text{rot}}) \end{cases}$$

$$\begin{cases} M \frac{d\mathbf{u}}{dt} = \mathbf{F} + M\mathbf{g} \\ I \frac{d\mathbf{\Omega}}{dt} = \mathbf{T} + M\mathbf{g} \cdot (\mathbf{x}_c - \mathbf{x}_{\text{rot}}) - k_d \cdot \mathbf{\Omega}_k \end{cases}$$

$$\frac{d\mathbf{x}_i}{dt} = \mathbf{u} + \mathbf{\Omega} \times (\mathbf{x}_i - \mathbf{x}_{\text{rot}})$$

Contents

One

background

Two

Methodology

Three

Results& discussions

Four

Conclusions



Results& discussions

Contents

One
background

Two
Methodology

Three
Results& discussions

Four
Conclusions

3.1 Standing Waves

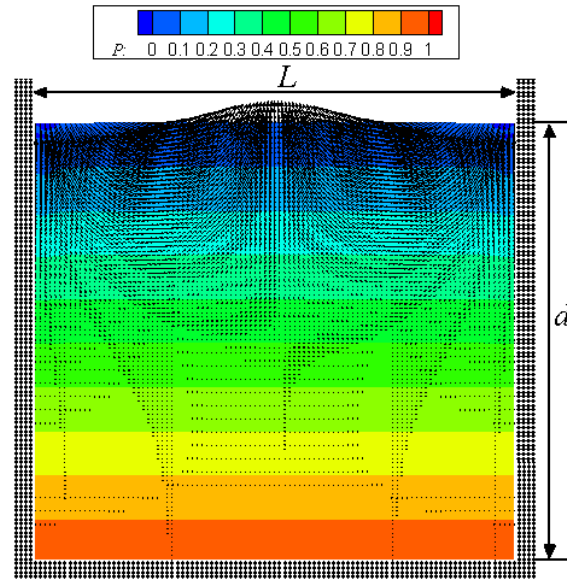


Fig.1 Tank model and its initial condition

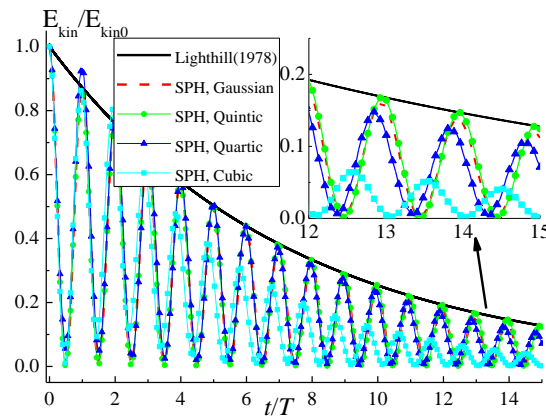
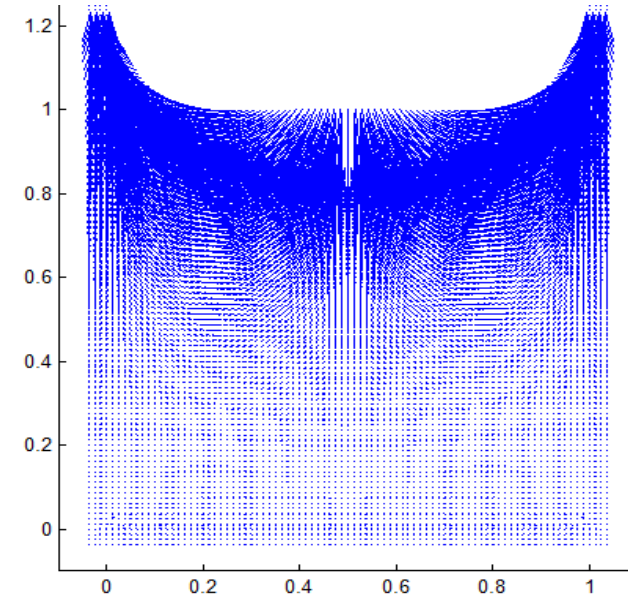


Fig.2 Effect of kernel functions on results

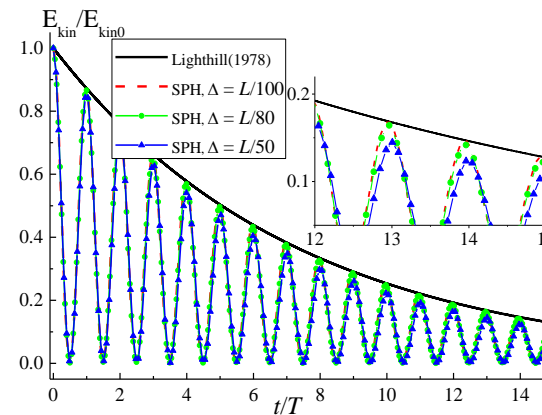


Fig.3 Effect of spacing resolutions (Gaussian)

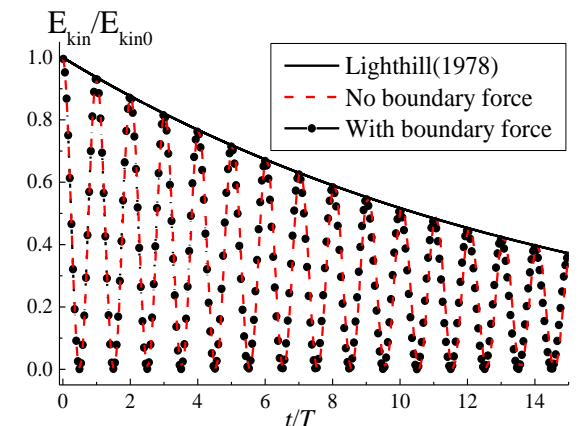


Fig.4 Effect of the boundary force model

Contents

One
background

Two
Methodology

Three
Results& discussions

Four
Conclusions

3.2 Wave tank

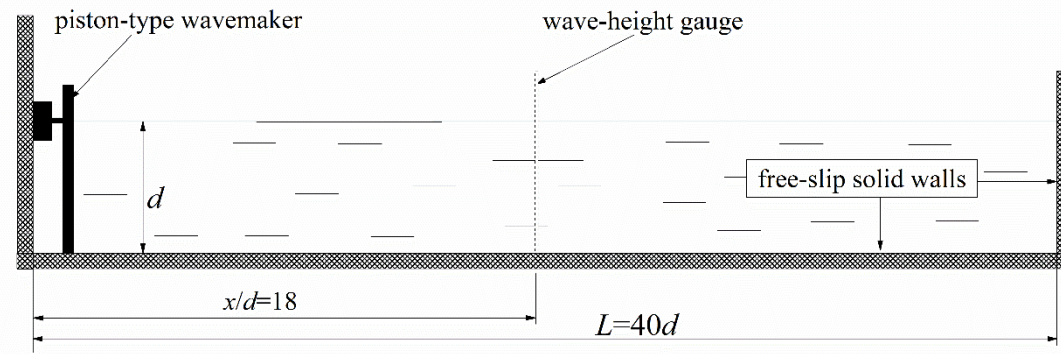


Fig.1 The sketch of numerical wave tank

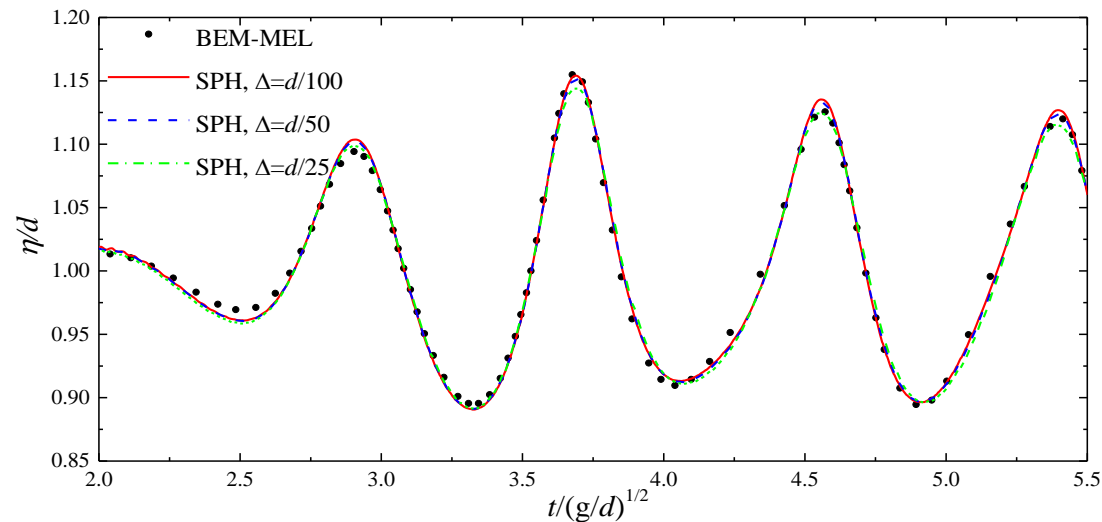


Fig.2 time profiles of water surface elevation predicted by different resolutions

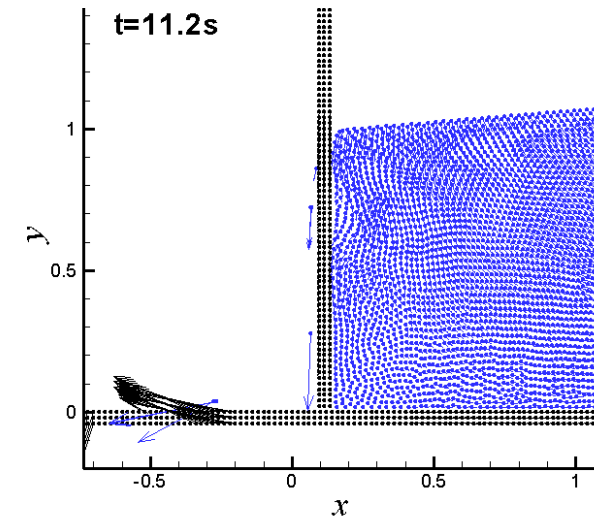
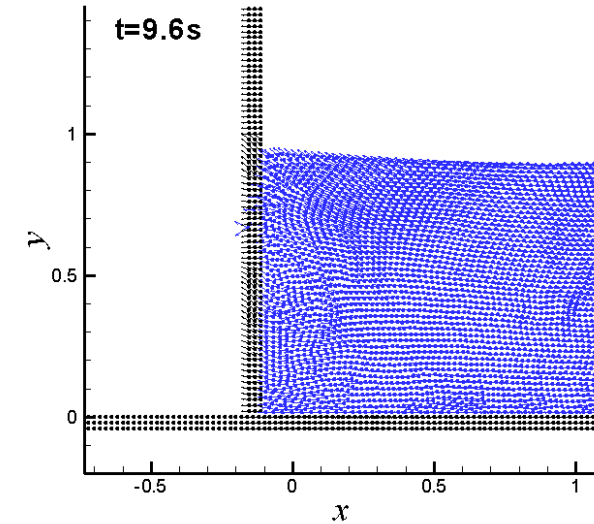


Fig.3 particles penetrate across the wall boundary

Contents

One
background

Two
Methodology

Three
Results& discussions

Four
Conclusions

3.3 Interaction of Wave & Rigid Plate

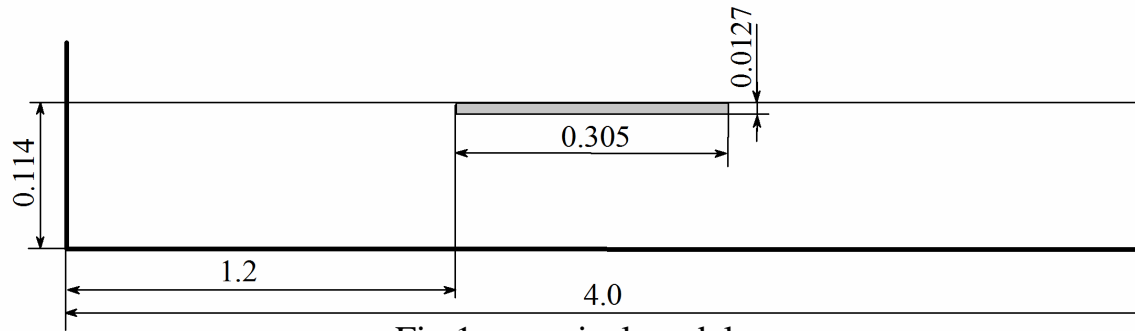


Fig.1 numerical model

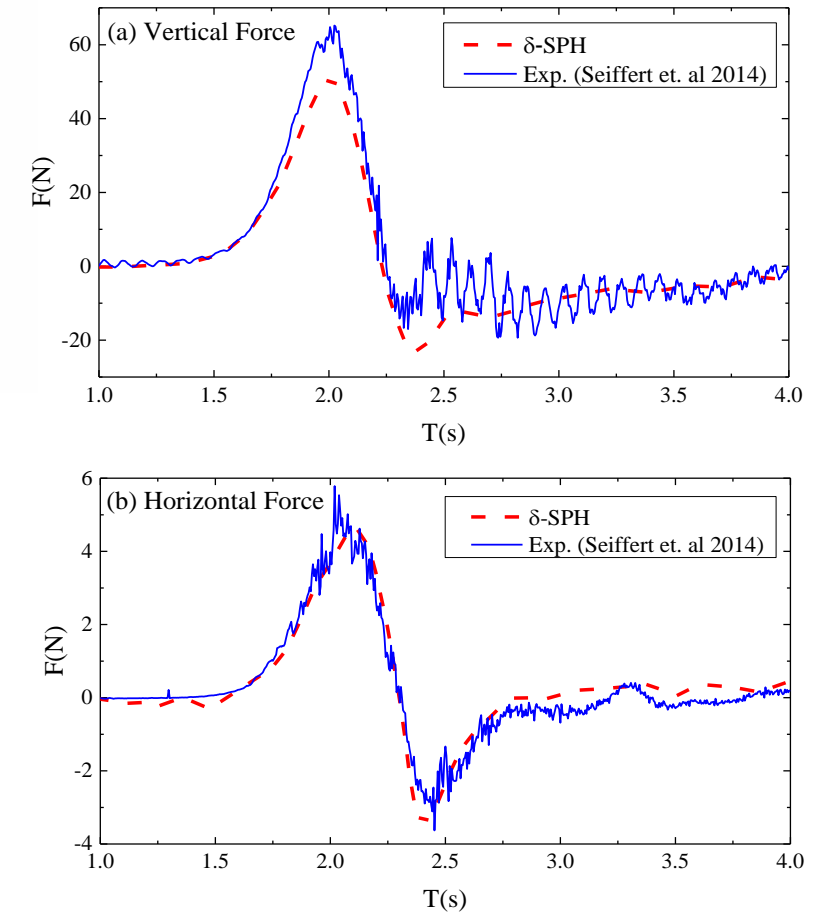
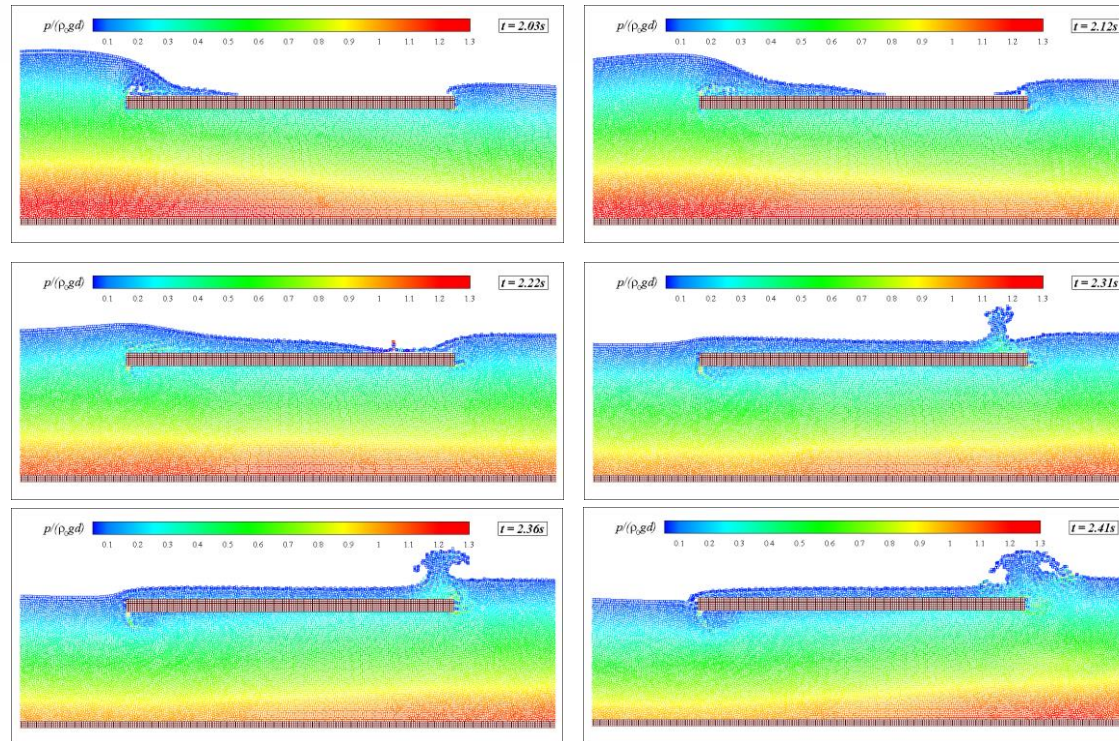


Fig.3 Comparison of the wave force on plate.
(Top: vertical force, Bottom: horizontal force.)

Contents

One
background

Two
Methodology

Three
Results& discussions

Four
Conclusions

3.4 Flap-type WEC of bottom-hinged pivot

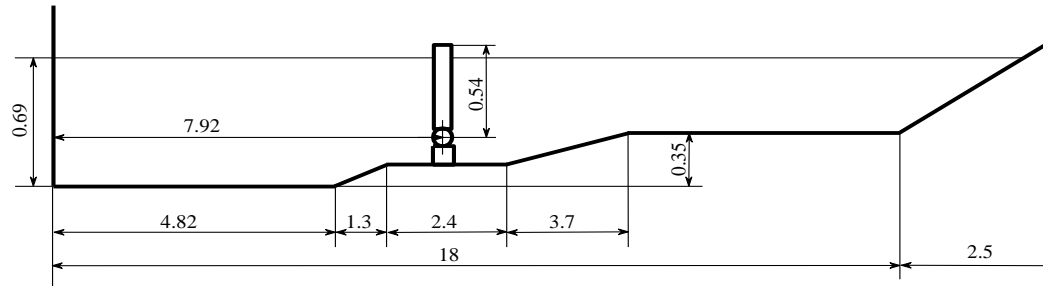


Fig.1 The schematic of bottom hinged Oscillating Wave Surge Converter

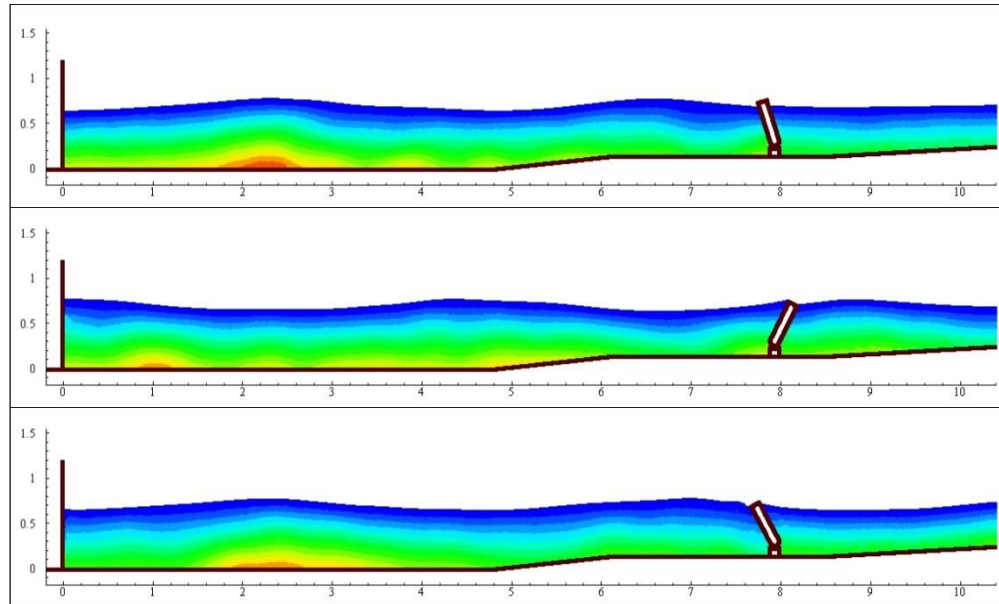


Fig.2 Pressure contours at different time.
(From top to bottom: $t = 5s$, $t = 6s$, $t = 7s$)

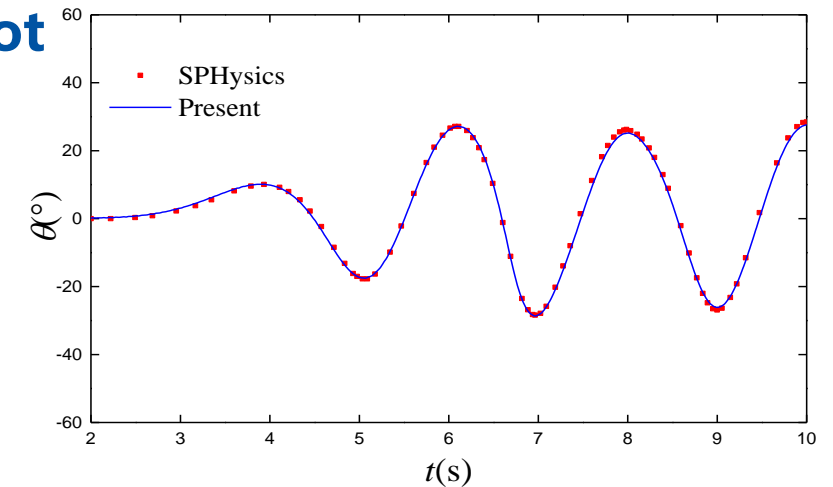


Fig.3a Time histories of the flap rotation angle
(no damping)

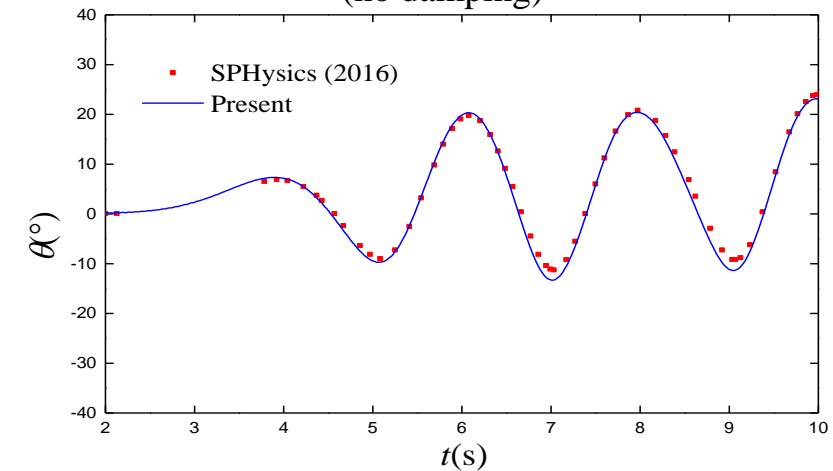


Fig.3b Time histories of the flap rotation angle
(damping $k_d = 35$)

Contents

One
background

Two Methodology

Three

Results & discussions

Four Conclusions

The diagram illustrates the experimental setup for wave motion measurement. It shows a rectangular tank with a wave maker on the left and a supporting fixed frame on the right. A floating body is positioned in the center. The wave maker is at a distance x_r from the floating body. The floating body is pivoted at a center, with a vertical distance z_r from the bottom. The water depth is 0.8m. The total length of the tank is 40m. The coordinate system (x, z) is shown at the bottom left.

Fig.1 The schematic of land hinged Oscillating Wave Surge Converter

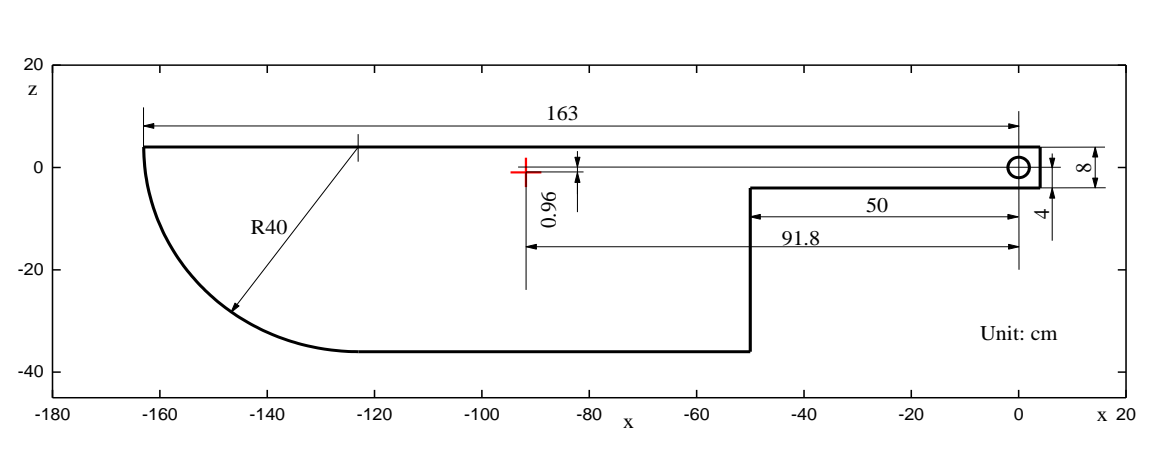
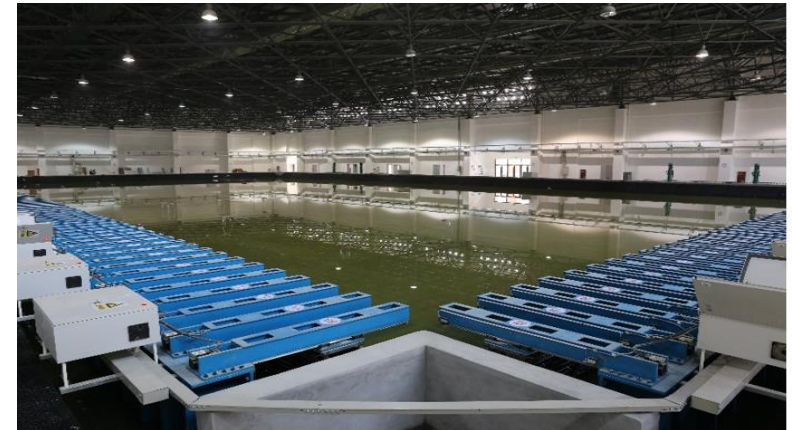
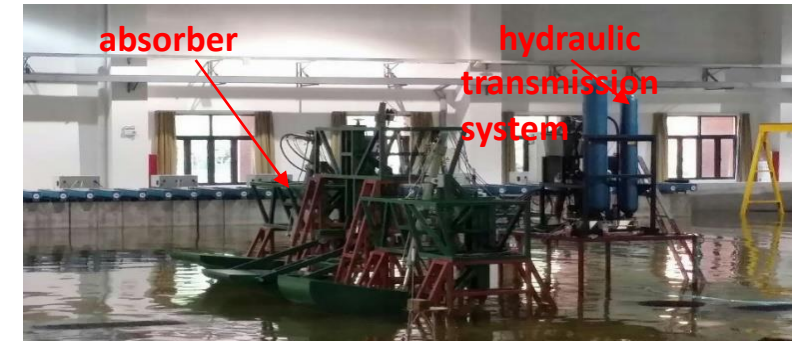


Fig.2 The sketch of pivoted absorber.



Contents

One
background

Two
Methodology

Three
Results& discussions

Four
Conclusions

3.5.1 Single absorber

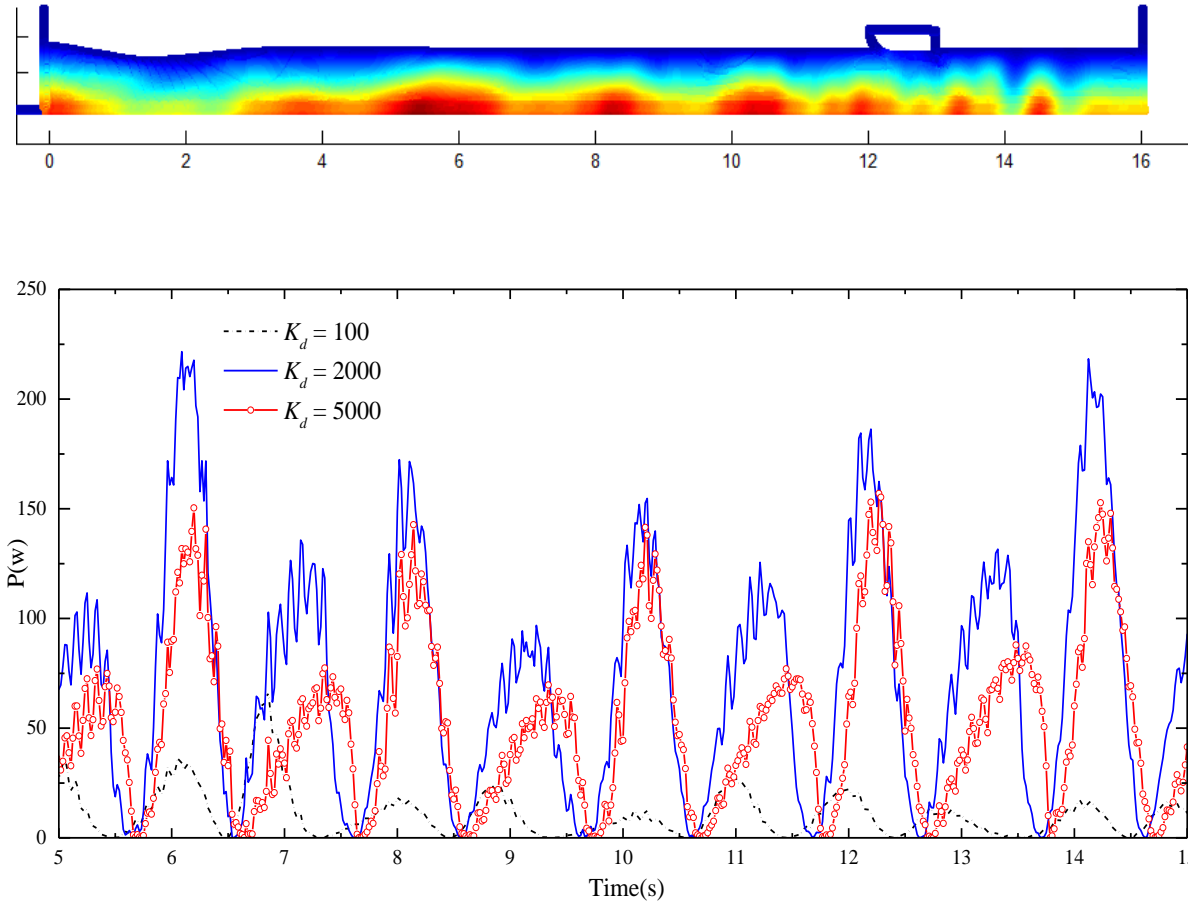


Fig.1 The instantaneous power of absorber with different PTO damping coefficients

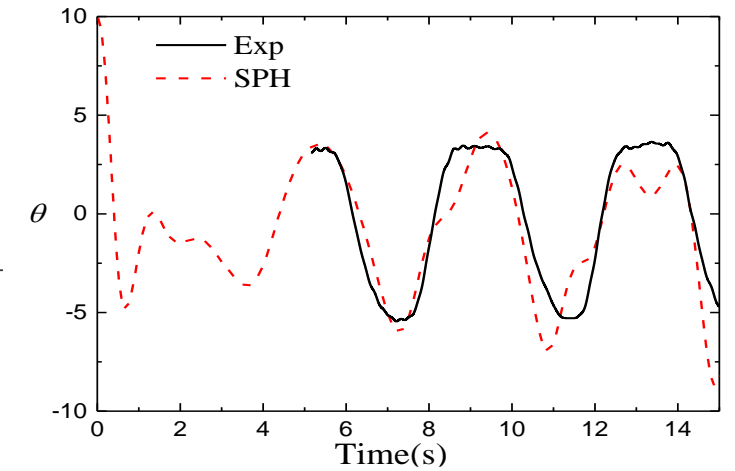


Fig.2 Comparison between SPH and experiment under period $T=4s$

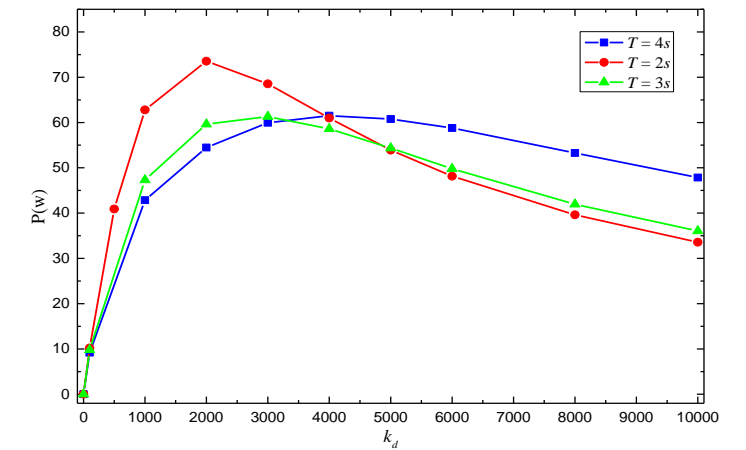


Fig.3 The active power of absorber with different PTO damping coefficients for different wave periods

Contents

One
background

Two
Methodology

Three
Results& discussions

Four
Conclusions

3.5.2 Double absorber

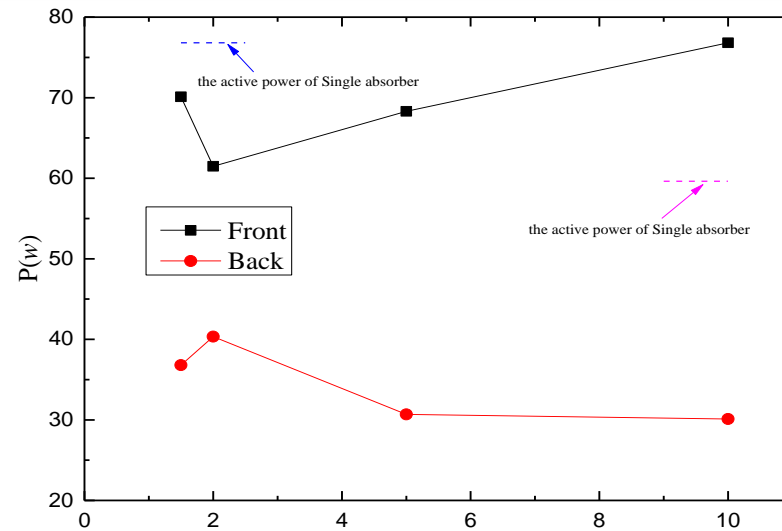
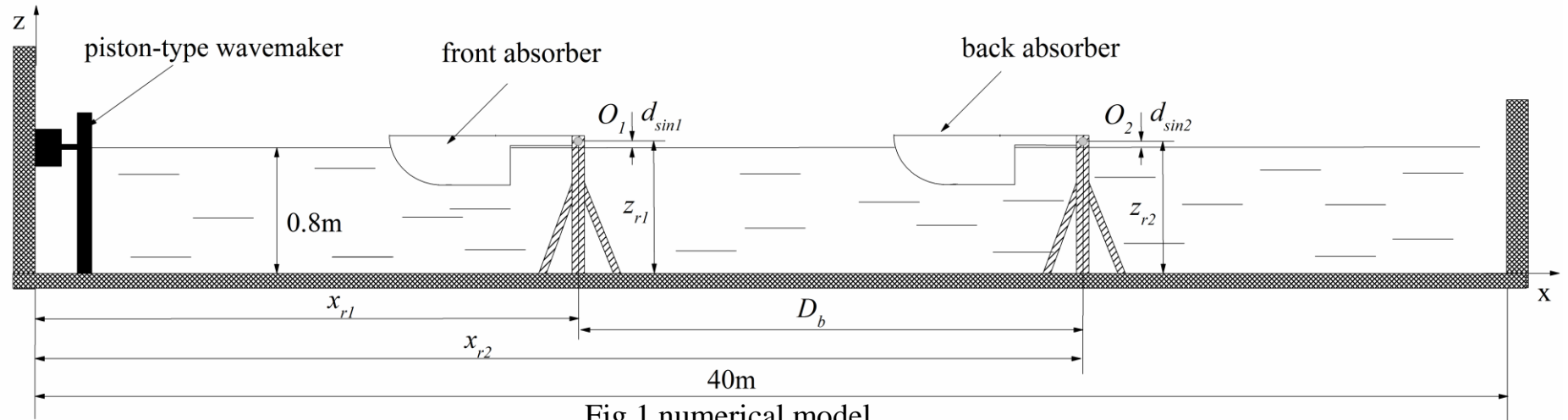


Fig.2 The active power of absorbers with different gaps

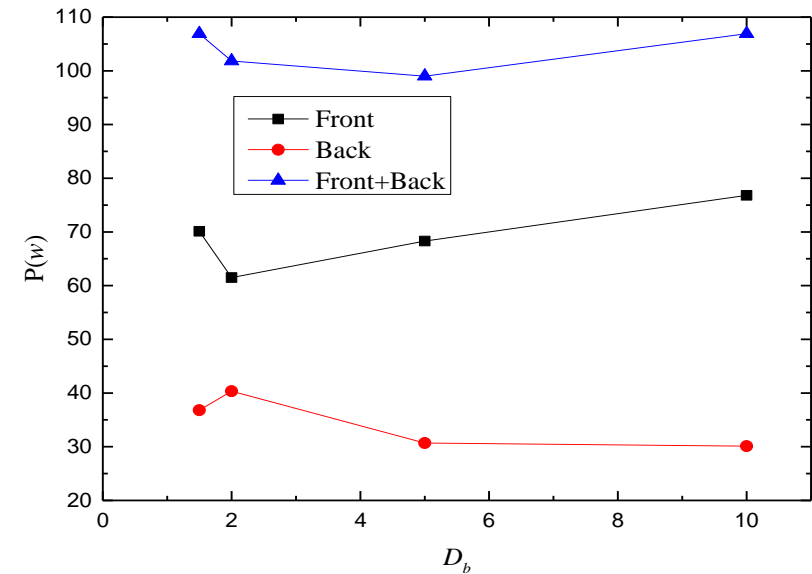


Fig.3 The total active power of absorbers

Contents

One

background

Two

Methodology

Three

Results& discussions

Four

Conclusions



Conclusions

Contents

One

background

Two

Methodology

Three

Results& discussions

Four

Conclusions

Conclusions

1

The selection of kernel function is critical for accuracy of SPH method. Gaussian kernel can be regarded as a proper kernel function for simulations of waves.

2

The PTO damping coefficients and the wave periods have important effect on active power, and there is the optimal damping coefficient for the fixed wave period.

3

The distance between two absorbers has large effect on energy capturing efficiency, and the maximal active power is obtained when the distance is large enough.



Thanks_{for} Your Attention

ZheJiang University
Shi Yingxuan